Geofísica Internacional (2004), Vol. 43, Num. 2, pp. 241-249

Cosmic rays and trapped protons as a source of the Earth's positron radiation belt

A. A. Gusev[1], U. B. Jayanthi[1], V. M. Pankov[2], G. I. Pugacheva[3] and N.G. Schuch[3]

[1] *Instituto Nacional de Pesquisas Espaciais, INPE, São Jose dos Campos, SP, Brasil,*

[2] *Space Research Institute of Russian Academy of Science, Moscow, Russia*

[3] *Southern Regional Space Research Center/INPE, Santa Maria, Brazil*

Received: March 31, 2002; accepted: July 18, 2002

RESUMEN

Se discute la posible existencia de un cinturón de radiación de positrones en la magnetosfera interior, su localización, su flujo y distribución de energías y la razón de e^+/e^-. Sugerimos que la generación de positrones es debida al decaimiento de piones cargados que nacieron en las reacciones nucleares del cinturón de protones atrapados y de los rayos cósmicos primarios con la atmósfera residual a alturas de 100 a 1000 km sobre la superficie terrestre. Se hace una comparación con datos recientes proporcionados por el experimento AMS a bordo del transbordador espacial.

PALABRAS CLAVE: Rayos cósmicos, electrones atrapados, cinturones de radiación.

ABSTRACT

The possible existence of a positron radiation belt in the inner magnetosphere of the Earth, its space localization, flux and energy distribution and the ratio of e^+/e^- flux are considered. We suggest for the positron generation the decay of charged pions born in nuclear reactions of the trapped radiation belt protons and of primary cosmic rays with residual atmosphere at the altitudes of 100 to 1000 km over the surface of the earth. A comparison is attempted with the recent data of AMS experiment on board the space shuttle.

KEY WORDS: Cosmic rays, trapped protons, radiation belt.

INTRODUCTION

Nuclear interactions of cosmic ray protons with the Earth's atmosphere are a well known source of charged and neutral energetic particles in magnetosphere. These interactions take place in the innermost region of the magnetosphere where the atmosphere still has a density sufficiently high to produce a noticeable number of secondaries and sufficiently low to permit these particles to escape from the atmosphere. The strength of the geomagnetic field in this region is practically the same as that at the Earth's surface and the influence of this relatively strong magnetic field on the secondary charge particle fluxes produces several significant geophysical effects. The most noticeable of them is the energetic ($\gtrsim$ 30 MeV) proton radiation belt created through the decay of energetic secondary neutrons escaping from the atmosphere (Cosmic Ray Albedo Neutron Decay - CRAND).

Charged secondaries born in the atmosphere and those that escape immediately are registered at satellite altitudes as albedo; splash, re-entrant and quasitrapped ones. The dependence of the primary cosmic ray flux on the cut-off rigidity (R_c) results in an increase of the intensity of the secondaries (both charged and neutrals) with latitude. Additionally, the cosmic ray cut-off rigidity depends on the angle of incidence with respect to the geomagnetic equator line at the same longitude. This azimuthal dependence of the primary cosmic ray flux in turn exhibits azimuthal dependence of secondary fluxes.

The trapped energetic protons of the radiation belt also interact with the residual atmosphere and generate further secondaries. These trapped particles can form new components of the radiation belt, including, for example, the isotope radiation belts. The species and spectra of the fluxes of the secondary radiation produced by the primary cosmic rays and the trapped proton radiation differ. Hereafter, to distinguish between the origin of these secondaries, the cosmic ray source and trapped proton sources are referred to as CR and TP respectively.

Freden and White (1960) were the first to point out the possibility that energetic TP can generate light element isotope ions like D, T, ^{3}He which could be trapped. This hypothesis of isotope radiation belt was confirmed experimentally by the observations of SAMPEX and CRRES satellites (Selesnik and Meawald, 1996; Chen *et al*., 1996; Spjeldvik *et al*., 1998a,b). Earlier, Basilova *et al*., (1982) considered

the energetic TP as a source of tens to hundreds MeV trapped electrons in the inner zone and this offers explains to their observations and subsequent results of Galper *et al*., (1983); Voronov *et al*., (1987). A natural consequence of this hypothesis is an existence of the positron radiation belt too (Gusev *et al*., 1996).

The simulations made to obtain absolute fluxes of secondary trapped positrons and electrons with rigidities less than ~8 GV/c, the minimal cut-off rigidity in the equatorial region, are presented here. As we consider relatively low energetic particles, these can not escape from the magnetosphere and perform a total or partial longitudinal drift around the Earth. In our earlier estimates of the trapped positron and electron fluxes of this nature (Gusev *et al*., 2001), we utilized essentially approximate and averaged parameters of nuclear reaction kinematics (averaged and approximated energy and angle distributions of secondary particles), and attempted normalized relative particle fluxes, etc. Here, we model the positron radiation belt flux in the inner Earth's magnetosphere after cosmic rays and protons of radiation belt utilizing more precise energy and angular distributions for the secondary products of the nuclear reactions of CR and TP with the residual atmosphere. We also consider the possible geophysical effects.

POSITRON FLUX FROM THE TRAPPED PROTON SOURCE

Both positrons and electrons from nuclear reactions of energetic protons with the nuclei of the residual atmosphere are presumed to be produced through the chain of decays of pions:

$$\pi^{\pm} \rightarrow \mu^{\pm} + \nu; \quad \mu^{\pm} \rightarrow e^{\pm} + \nu + \tilde{\nu} \qquad (1)$$
$$\pi^{0} \rightarrow 2\gamma \rightarrow 2e^{+} + 2e^{-} \ .$$

The energy threshold of incident proton for π meson production is ≈ 290 MeV.

Due to the very short life time of pions and muons the electrons are generated close to the point of nuclear interaction. Thus, the electrons and the positrons produced in the nuclear interactions will be essentially confined to the same *L*-shells of the parent energetic trapped protons. In contrast the γ-quanta from the decay of π^0 travel a long distance from the point of generation and not being affected by the geomagnetic field escape from the magnetosphere or sink in more dense atmosphere and don't contribute to the electron flux produced by TP.

To simulate a nuclear reaction yield, we initially computed the pion production spectra (originated in 1 g/cm^2 of atmospheric matter) using a well tested version of the Monte Carlo computer code SHIELD for the intra-nuclear cascade simulations (Dementyev and Sobolevsky, 1999). As a result we obtained distributions of pion output versus energy and angle in the laboratory system. Later, the muon energy distributions were obtained by decreasing the pion energy by a coefficient of 0.8, corresponding to the average part of the energy carried away by muon in π–μ decay. In the muon rest system the angular distribution of the decay electrons is isotropic and their energy spectrum normalized for one electron is described as $dN_e/dE_e = 1.347 \cdot 10^{-5} E^2 (3.0–4.0\ E/mc^2)$, MeV^{-1}, where E in MeV (Barashenkov and Toneev, 1972). To calculate the positron/electron production spectra the distributions were transformed with relativistic transformations from the muon rest system to the laboratory system considering the energy and angle of each muon.

In Figure 1, we show the positron excess as obtained in the computations of the positron/electron production spectra generated by protons of various energies (Gusev *et al*., 2001). For incident protons at energies in the range of 0.3 to 2.0 *GeV* and at electrons with energies of about 10 *MeV*, the ratios of the integral production fluxes are > 2 and have maximum value of ≈ 9 near 300 *MeV* the reaction threshold energy of proton. For proton of energies of ~ 0.5 to 2.0 *GeV,* this ratio increases up to a value of about 10 with increasing positron energy. Qualitatively, this result is a direct consequence of the charge conservation law which tends to favor

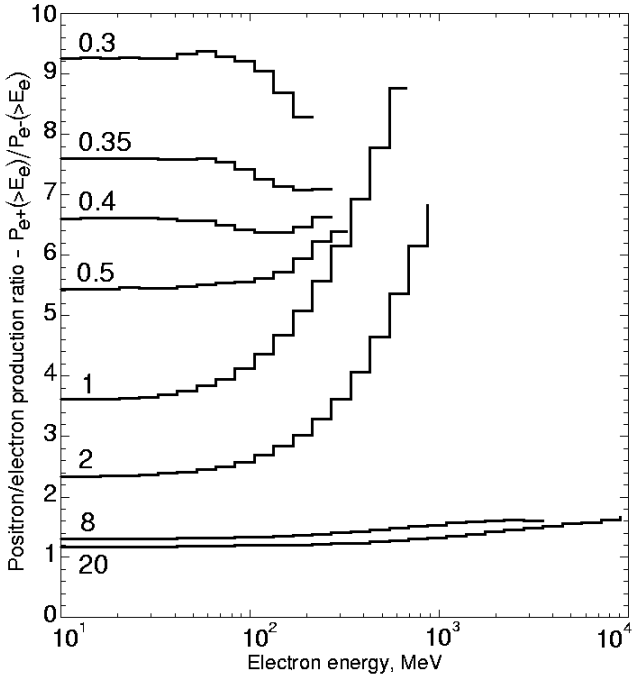

Fig. 1. The dependence of positron/electron production spectra ratio P_{e+} (>E)/P_{e-} (>E) on electron energy. Numbers near the curves mark an incident parent proton energy in GeV.

positive pion production when only a few pions are born in the nuclear reactions p + A → D+π^+ + A'; p+π^+ + A', and p+n+π^+ + A' predominating near the incident proton reaction threshold energy (Machner and Hidenbauer, 1999) (here A is a target atomic number and A' is the number of exited nucleus after reaction).

Thus, nuclear reactions of the trapped proton component with 0.3-2 *GeV* energy substantially favor the production of positrons over electrons in the energy range of about 10 *MeV* to several hundreds *MeV*. This important feature is quite unlike the situation for the CR protons in the geomagnetic equatorial region. These protons with minimal energy of ≈ 8 *GeV*, produce a greater number of pions and consequently the ratio of positron to electrons is almost equal to unity (see Figure 1, curves for proton energies 8 and 20 *GeV*).

Because the trapped proton component has significantly greater intensity in comparison with CR protons, at least at L-shell of 1.2, and especially near the reaction threshold, the TP source could predominate over the CR source, and provide enhanced trapped positron fluxes in comparison to electrons. The characteristics of the TP source extracted from AP8 model (AP8, 1996) for *L* shell of 1.2 are shown in Figure 2. The energy spectrum is very steep and indicates a break at energies of ~ 800 *MeV* and the angular distribution of the flux is relatively narrow ~18° near the geomagnetic equatorial plane.

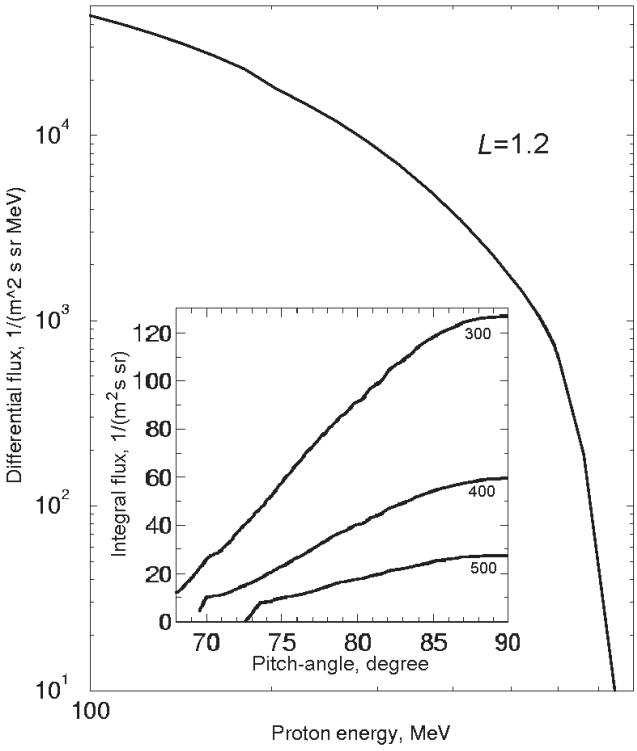

Fig. 2. The source spectrum of the trapped protons at *L*-shell of 1.2.

In Figure 3 we show an example of differential production spectra $P_{e+}(E'_e)$ of positrons generated by unidirectional TP flux. Although the resulting angle distribution of production fluxes is approximately isotropic, only those positrons which have the same pitch angles as the trapped parent protons will be captured by the magnetic field. A pitch-angle corresponding to the loss cone at L=1.2 is about 70°, thus the solid angle of confinement region at L=1.2 is equal to 1.4 π sr.

To calculate the positron/electron differential flux $F_{e\pm}(E_e)$ we must integrate the differential production spectrum $P_{e\pm}(E'_e)$ along the positron trajectory considering that positron of energy E_e was born with energy E'_e at a distance of X' g/cm^2 from the point of observation. Then the positron flux of energy E_e at the point of observation is determined by the particle conservation law which can expressed as:

$$F_e(E_e)\Delta E = \int_0^\infty P_e(E'_e, X')\Delta E'(E_e, \Delta E, E'_e(X'), X')dX', \qquad (2)$$

where $\Delta E'(E_e, \Delta E, E'_e(X'), X')$ is a function describing the variation of the energy interval ΔE with changing energy along the positron trajectory.

As shown by Pugacheva *et al.*, (1997), as the production spectrum P_e and the positron/electron energy losses (dE/dX) do not depend on X' (i.e. the both depends only on E'_e) then the integral (2) reduces to

$$F_e(E_e) = \frac{P_e(> E_e)}{\left(\frac{dE}{dx}\right)_{E_e}}, \qquad (3)$$

where $P_e(>E_e)$ is an integral positron/electron production spectrum.

The total energy losses of energetic positrons trapped in the inner radiation zone are given by:

$$\frac{dE}{dx} = 0.002 + 0.028E + 3.86\cdot 10^{-6} E^2 B^2 / c\bar{\rho}, \quad GeV/(g/cm^2). \qquad (4)$$

Here the first and second terms represent the ionization and bremsstrahlung losses (Yuan and Wu, 1961), and the third term is the synchrotron radiation energy loss (with $\bar{\rho}$ as the mean atmospheric density along the electron drift trajectory around the Earth), (Ginzburg, 1987). The synchrotron radiation losses are negligible only in the region very close to the Earth. At the magnetic equator along the field line L=1.2 where B=0.312L^{-3}=0.18 *Gauss*, and $\bar{\rho}\approx 10^{-17}$g/cm^2 synchrotron radiation energy losses surpass the ionization and bremsstrahlung losses: $(dE/dx)_{synchr} \geq (dE/dx)_{ion+brem}$ for

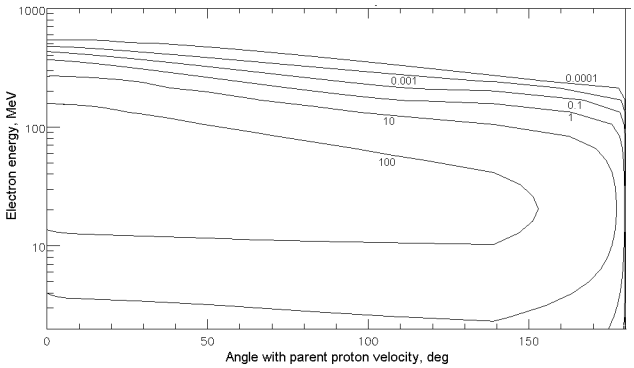

Fig. 3. The angle-energy distribution of positrons produced in π→μ→e decays. Numbers near the curves indicate the differential positron production flux in units positrons/MeV s sr g.

electrons with an energy of > 100 MeV. For L ≤ 1,2 *dE/dX* depends only on *E* in the flux calculations. The results of the simulations are presented in Figure 4. Taking into account that the trapped protons with energy more than 300 MeV has maximum intensity at $L \sim 1.2$ we can conclude that the geomagnetically trapped positron flux is expected to reside in a narrow belt with maximum near *L*=1.2. A characteristic feature of this source of trapped positrons is a high e^+/e^- ratio, around 7-8, for the positrons of 10 - 500 MeV.

TRAPPED POSITRON FLUX FROM THE COSMIC RAY SOURCE

CR protons also produce positrons and electrons in nuclear reactions with the residual atmosphere which can be trapped at the same L-shells where TP generates positron radiation belt. One can expect lower trapped positron fluxes from CR source due to its low intensity at the same L-shells, as for example, at L=1.2 where CR flux is the 5-6 orders of magnitude less in comparison with TP flux there. However, the multiplicity of pions produced by CR protons of tens of GeV is greater than that due to 300 MeV TP component. As the pion production spectrum is a result of source flux and multiplicity, it is not so obvious how many absolute values of trapped positron fluxes generated by TP will exceed those produced by CR at the same L-shells. The modeling of a positron radiation belt with the estimation of e^+/e^- flux ratio was first performed for L-shells 1.09, 1.12 and 1.2, taking into account the arrival directions of CR parent fluxes in Pugacheva *et al.*, (2001), but the meeting didn't published presentations.

Figure 5 shows the parent proton CR spectra used for the simulation of secondary positrons/electron fluxes at these L-shells (AMS collaboration, 2000a). CR spectra at low latitudes depend on CR arrival direction, i.e. on the angle of their velocities with the eastern direction, so called azimuthal asymmetry in CR flux. The spectra in Figure 5 correspond

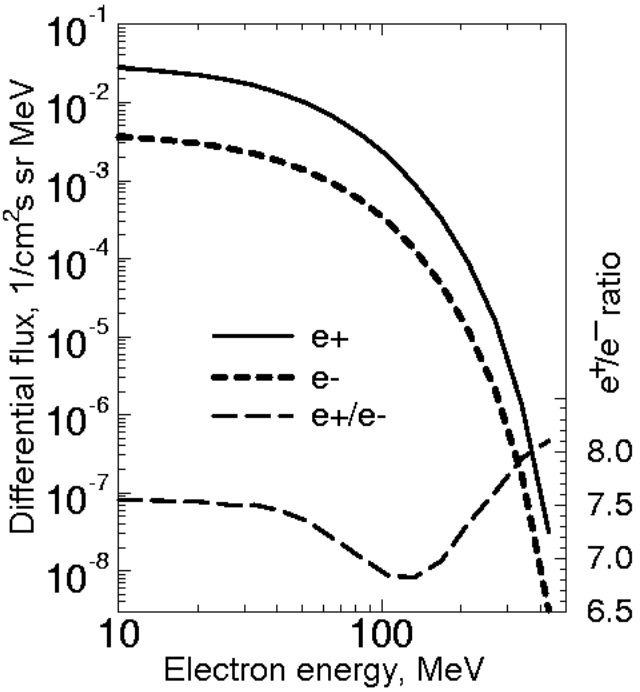

Fig. 4. Spectra of the trapped positrons and electrons produced by trapped proton source.

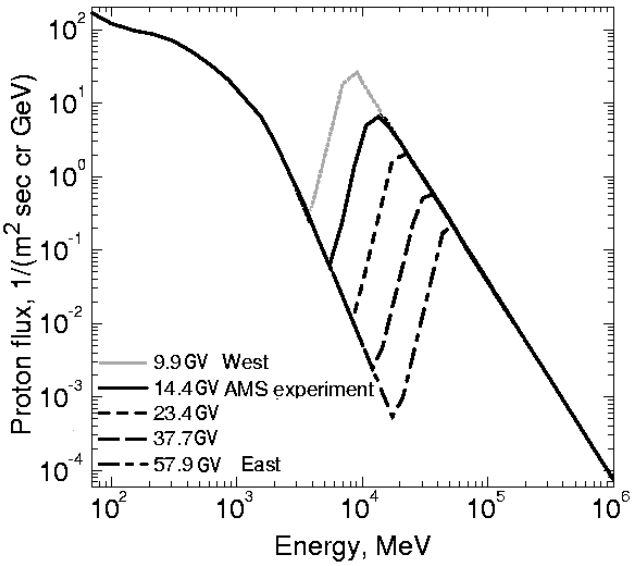

Fig. 5. Experimental parent proton spectra for the geomagnetic equator region at L = 1.09 in dependence of arrival direction. The spectra consist of the primary and secondary components.

to different cut-off rigidities determined by arrival direction of CR flux. The spectrum sums secondary and primary components. The measurements were performed by Alpha Magnetic Spectrometer (AMS). AMS is a high energy physics experiment scheduled for installation on the International Space Station for antiparticle - antimatter measurements. In preparation for this mission, AMS flew a precursor mission

on board the space shuttle Discovery in June 1998. Here and below we refer to the numerous results of the flight.

At energies below 3 GeV the spectrum consists of secondaries which are independent of rigidity due to local production. The primary components depend on the rigidity where higher the rigidity, the lower is the flux: $F(>R_c) \geq 7000/(R_c)^{3/2}$. The CR protons arriving from the western direction have about 14 times higher intensity compared to those arriving from eastern direction.

The positrons and electrons are mostly produced in nuclear reactions at the lowest atmospheric altitudes that the geomagnetic equatorial line related to a certain L-shell reaches. The minimal altitude (H_{min}) of the geomagnetic equator line of L-shell of 1.09 is ≈ 80 km which corresponds to the atmospheric boundary, i.e. it is the first closed L-shell where charged particles could be captured by magnetic field in the sense to make at least one drift rotation around the Earth. The equatorial lines of L=1.12 and L=1.2 have H_{min} at 250 km and 800 km respectively. Particles with pitch angles about 90° drift along the geomagnetic equator around the Earth, with the positrons and electrons drifting in opposite directions due to radial gradients in the geomagnetic field. Figure 6 shows how positrons and electrons produced by the western CR protons drift along the geomagnetic equator line of L=1.06 (broken line) from the production region. The upward moving particles can escape from the atmosphere and reach satellite altitudes, the downward moving particles sink into the atmosphere and are lost.

One must pay attention that the upward drifting electron produced by westward CR has their guiding center beneath the production point, when the positrons above it. The positrons pass through the more rarified atmosphere and the electrons which encounter denser atmosphere in comparison suffer higher energy losses impeding their escape from the atmosphere. This effect illustrated in Figure 7, where simulated trajectories of a positron and an electron starting from the atmospheric boundary are sketched. One can see that only the positron escapes from the atmosphere. The higher the electron energy, the deeper it sinks into the atmosphere and more rapidly is lost.

If the particles are produced by eastward moving protons the effect is the opposite *i.e.* only electrons escape from the atmosphere, but, however, their flux is significantly lower due to the significantly lower intensity of parent eastward CR protons. In the intermediate case of vertical incident CR protons the electrons and positrons escape from the atmosphere in a similar manner.

These considerations led us to employ Equation (2) rather than the Equation (3) for the absolute flux simulations as the production spectrum changes along the particle trajectory due to the dependence of the cut-off rigidity of the CR protons on arrival direction. The integration of Equation (2) is performed over the quantity of the matter that a particle encounters along the trajectory. Due to that the maximal input to the Integral (2) comes from the lower part of the Larmor circles passing through the denser atmosphere. As

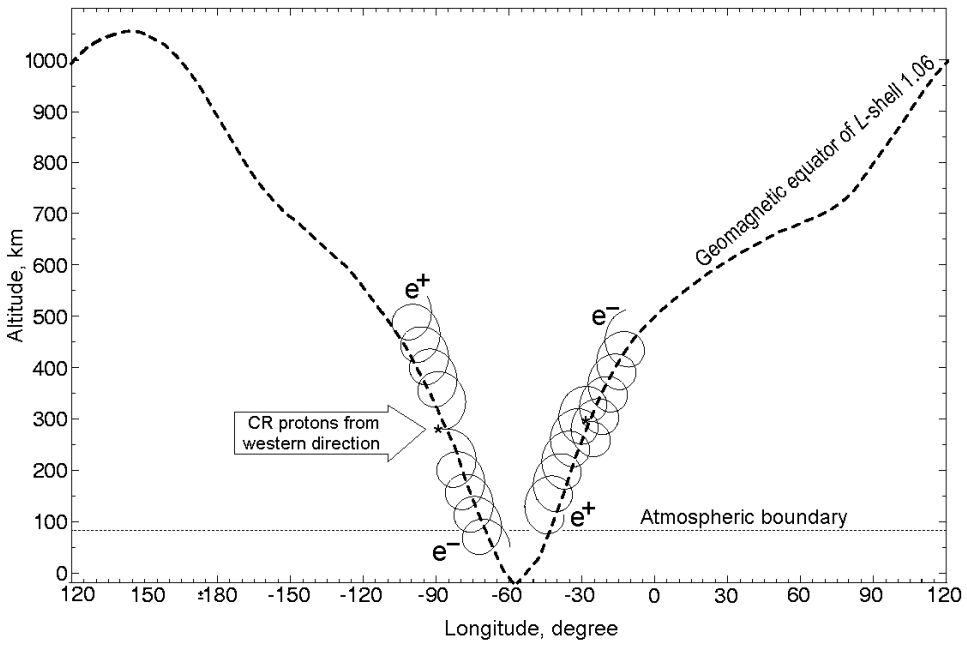

Fig. 6. Drift of the positron and electrons generated by western protons along the geomagnetic equator at unclosed L=1.06.Energy losses in the atmosphere are not taken into account in the figure.

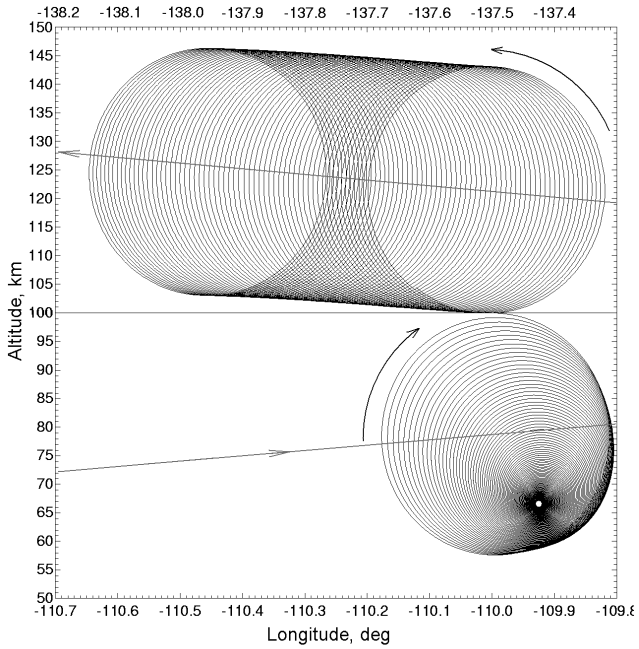

Fig. 7. Simulated trajectories of a positron and an electron born at the same point at the altitude of 100 km, drifting upward along the geomagnetic equator with the guiding centers above (for positrons) and beneath (for electrons) the point of generation. The curved arrows show direction of Larmor rotation. The straight lines with the arrows show the geomagnetic equator line and magnetic drift direction.

seen in Figure 7, in the bottom of the Larmor circle the velocity of an escaping positron is directed to the east. As secondary particles are mainly produced by CR in the direction of the incidence, these escaping eastward positrons are produced mostly by westward CR flux. As the westward CR flux is higher it produces higher input to the integral secondary particle flux compared to the input from the eastward directed CR protons. For the escaping electrons the effect is the opposite; input in their flux from the eastward CR is higher than from the westward directed. But eastward CR fluxes are less intense than the westward and consequently the secondary fluxes produced by the eastward CR are lower. The greater the difference between the densities at the top and at the bottom of the Larmor radius, the greater is the difference between the positron and electron fluxes.

Figure 8 demonstrates an angle-energy distribution of the electrons generated by CR. The distribution has a noticeable anisotropy for electrons with energies ≥ 40 MeV and has a maximum in the direction of the parent proton and permits simplification by assuming that in the case of CR production all the secondary positrons move in the same direction as the parent proton.

Figure 9 demonstrates results of simulations of trapped positron and electron fluxes at L=1.09 generated by CR and the comparison with the data of AMS experiment. The positron/electron fluxes at L-shells of 1.12 and 1.2 are not shown; they are approximately (within precision of 10 to 30%) the same as computed at L=1.09, because secondary fluxes are proportional to the CR intensity for closed L shells. We also show in Figure 9 the positron/electron fluxes modeled with the Equation (3) when an azimuthal asymmetry of CR is not considered. The simulation utilized the vertical CR spectrum observed by AMS at L < 1.09. There is an obvious difference in the results; when fluxes are simulated along the particle trajectories with Equation (2) then a significant positron excess is obtained; a positron excess is almost absent in the second case.

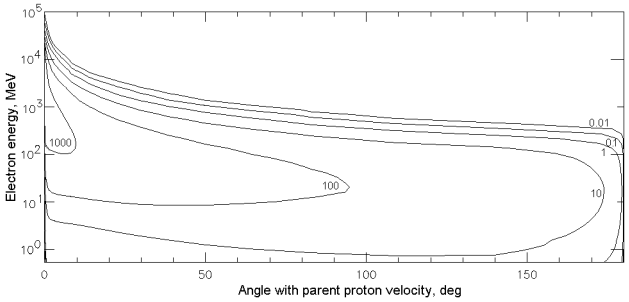

Fig. 8. The angle-energy distribution of positrons like in Figure 3 but produced by CR.

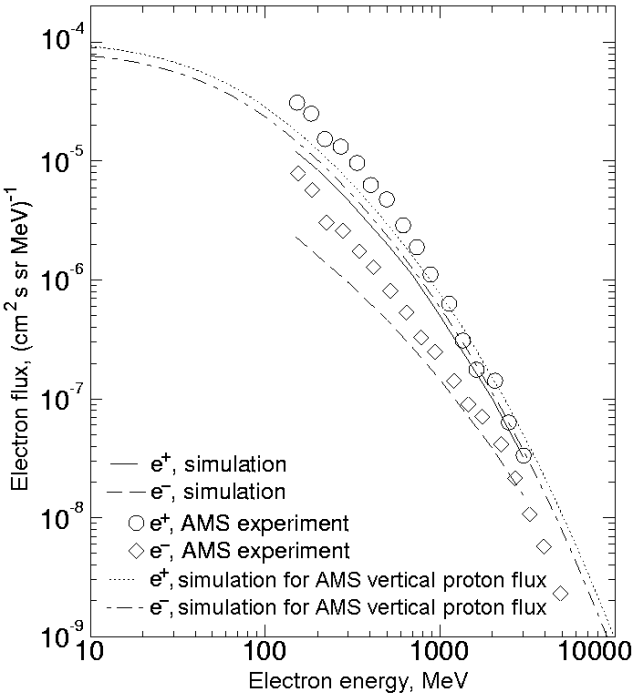

Fig. 9. The results of simulation of trapped positron and electron fluxes born by CR at L=1.09 and comparison with the data of AMS experiment.

Comparing the resulting trapped positron/electron fluxes from the TP and CR sources presented in Figures 4 and 9 one can confirm that the TP source creates about 100 times greater positron fluxes than the CR source at the same L-shell with energies less than 100 MeV. This exhibits sharply decreasing spectrum after 200-300 MeV. At these energies of ≥ 200 MeV, positron fluxes from the TP source are still comparable with the CR born positrons, but at greater energies this TP source is negligible in comparison with the CR source.

The quasi-trapped positron and electron fluxes at L< 1.09 observed in AMS experiment are essentially originate below 100 km of atmosphere (AMS collaboration, 2000b). Our simulation results and the observed AMS fluxes are in a good agreement at energies more than 700 MeV (Figure 8). At lower energies there still exists differences that possibly could be related to the next generation particles in the development of nuclear cascade in the atmosphere which we did not consider in our simulations the trapped flux at L=1.09. In our simulations we take into account only the secondary particles from the first interaction of primary protons with the atmospheric atoms. The probability of second nuclear interaction with the residual atmospheric atoms is proportional to the square of the atmospheric density and is very small for the atmospheric altitudes considered here (L=1.09 with H_{min} = 80 km; 1.12 with H_{min}=250 km; and 1.2 with H_{min}=800 km).

The positron excess was also clearly observed in AMS experiment for L < 1.09 in quasi-trapped positron/electron fluxes (Figure 11).

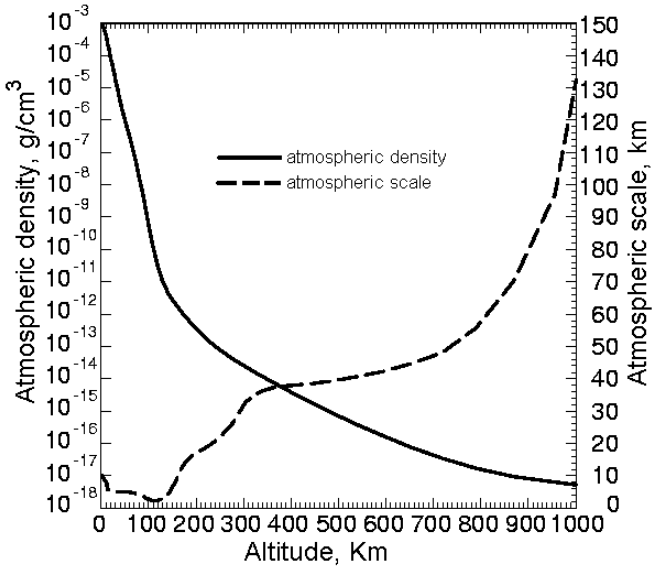

Fig. 10. Atmospheric density scale.

An essential condition for providing a difference between the fluxes of escaping positron and electrons is the rapid decrease of the atmosphere density which scales with the altitude. The positron excess can only be achieved if the atmospheric scale height is less or at least comparable with the Larmor radius of the secondary positron/electron. The atmospheric scale height increases with the altitude (see Figure 10). Thus the positron/electron ratio is dependent on the altitude of the trajectory of the escaping particles and so decreases with the altitude. It depends mostly on H_{min} of a given L-shell which contributes maximal input to the integral (2). This is noted in the computed positron/electron flux ratio at L=1.12 and L=1.2 which are significantly less than that at L=1.09 (Figure 11), essentially due to the atmospheric scale height increasing with the altitude and the role of CR azimuthal asymmetry is limited in the flux production.

CONCLUSIONS

The positron radiation belt flux in the inner Earth's magnetosphere is modeled after cosmic rays (CR) and protons of radiation belt (TP) interacting with the residual atmosphere in nuclear reactions and decays, at altitudes above 80 km. The spatial location and the fluxes at the top of magnetic field lines are given for both the sources. The simulations show that positron radiation belt fluxes from the assumed

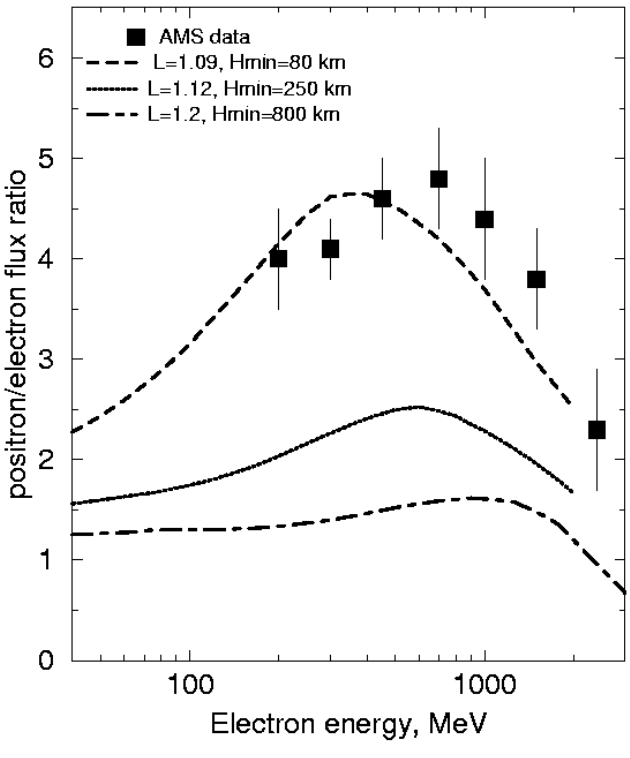

Fig. 11. Positron/electron flux ratio for CR source; circles are data of AMS experiment.

TP source are limited in spatial distribution at around L=1.2 ± 0.1 with the energy spectrum showing a steep cutoff at energy of about ~ 300 MeV. The calculated e^+/e^- flux ratios in the belt due to this source are high and attain values of ≥ 7 in the energy range of 10 to 500 MeV. The simulated results for the CR source, at the center of the positron belt, are about 100 times lower than the positron fluxes of the TP origin at L=1.2. The CR origin fluxes are also less in the space at L≥1.2 due to the strong synchrotron energy losses, but their fluxes continue practically equal down to L ~1, unlike the fluxes due to the TP source which are localized around at L=1.2. The estimated spectra due to the CR origin are flat and measurable fluxes could be obtained up to 2000 MeV energy. The calculations show that the e^+/e^- flux ratio due to the CR source reaches 4 – 5 for positrons trapped at first closed L shells such as L=1.09 decreasing to ~ 2 at L = 1.2. The lesser the positron energy the lesser are the e^+/e^- flux ratio due to the CR source. This is due to the combination of geophysical effects such as the variation in the atmospheric scale height with the altitude or rather the positron Larmor gyration radius comparable or even greater than atmospheric scale height and the azimuthal dependence of the CR fluxes producing anisotropic angular distribution of secondary particles born in nuclear reactions. The results of the positron belt modeling made here are in a reasonable agreement with AMS results, especially in the high energy range (> 700 MeV) of the positron spectrum.

ACKNOWLEDGEMENTS

Dr. A. Gusev was sponsored by the CNPq of Brazil, Dr. G. Pugacheva was sponsored by the FAPERGS, RS/Brazil. The authors thank ALAGE and the Organizing Committee of 6COLAGE

BIBLIOGRAPHY

AP8, http://nssdc.gsfc.nasa.gov/space/model/magnetos/radbelt.html, 1996.

BARASHENKOV, V. S. and V. D. TONEEV, 1972. Interaction of Particles and Atomic Nuclei of High and Superhigh Energies with Nuclei, Atomizdat, Moscow, Russia, 812pp.

BASILOVA, R. N., A. A. GUSEV, G. I. PUGACHEVA, A. F. TITENKOV, 1982. High energy trapped electrons in the inner radiation belt. *Geom. and Aeronom., 22,* 671-673.

CHEN, J., T. G. GUZIK, J. P. WEFEL, K. R PYLE and J. F. COOPER, 1996. Energetic helium isotopes trapped in the magnetosphere. *J. Geophys. Res. 101* (A12), 24787-24790.

DEMENTYEV, A. V., N. M. SOBOLEVSKY, 1999. SHIELD - universal Monte Carlo hadron transport code: scope and applications. *Radiation Measurements, 30,* 553-562.

FREDEN, S. C. and R. S. WHITE, 1960. Particle fluxes in the inner radiation belt. *J. Geophys. Res., 65(5)*, 1377-1383.

GALPER, A. M., V. M. GRACHEV, V. V. DMITRENKO *et al.*, 1983. High energy electrons in the radiation belt of the Earth, 18 Int. Cosmic Ray Conference, Bangalore, India, MG.10 33, 497-500.

GINZBURG, V. L., 1987. Theory of Physics and Astrophysics, Academy of Science, Moscow, Russia, 344.

GUSEV, A. A., I. M. MARTIN, G. I. PUGACHEVA, A. TURTELLI, Jr. and W. N. SPJELDVIK, 1996. Energetic positron population in the inner zone, *Il Nuovo Cimento, Sect. C, 19,* 461-465.

GUSEV, A. A., U. B. JAYANTHI, G. I. PUGACHEVA, W. N. SPJELDVIK, 2001. Nuclear reactions on rarest atmosphere as a source of magnetospheric positron radiation belt. *J. Geophys. Res., 106,* A11, 26111-26115.

MACHNER, H. and J. HIDENBAUER, 1999. Meson production close to threshold. *J. Physics G. Nuclear and Particle Physics, 25(10)*, 231-271.

PUGACHEVA, G. I, W. N. SPJELDVIK, A. A. GUSEV, I. M. MARTIN, 1997. On the natural energetic positron population in the inner zone of the Earth. *J. Atmosph. Sol. Terr. Phys., 59,* 363-369.

PUGACHEVA, G. I., W. GONZALEZ, A. A. GUSEV, U. B. JAYANTHI, I. M. MARTIN, D. BOSCHER, S. BOURDARIER and W. N. SPJELDVIK, 2001. Numerical simulation of steady state proton, positron, isotope ion radiation belts and of a sudden creation of transient helium radiation belt during geomagnetic storms, ISEC2001 Radiation Belt Science and Technology, July 23-27, 2001, Queenstown, New Zealand, [http://spacsun.rice.edu/ãac/isec2001/].

SELESNICK, R. S. and R. A. Mewaldt, 1996. Atmospheric production of radiation belt light isotopes. *J. Geophys. Res. 101 (A10)*, 19745-19759.

SPJELDVIK,W. N., G. I. PUGACHEVA, A. A. GUSEV, I. M. MARTIN and N. M. SOBOLEVSKY, 1998a.

Sources of inner Radiation Zone Energetic Helium Ions: cross-field transport versus in situ nuclear reactions. *Adv. in Space Res. 21,* 1675-1678.

SPJELDVIK, W. N., G. I. PUGACHEVA, A. A.GUSEV, I. M. MARTIN and N. M. SOBOLEVSKY, 1998b. Hydrogen and helium isotope inner radiation belts in the Earth's magnetosphere. *Ann. Geophys., 16,* 931-939.

VORONOV, S. A., A. M. GALPER, V. G. KIRILLOV-UGRYUMOV, S. V. KOLDASHEV and A. V. POPOV, 1987. High energy electrons and positrons in the Earth's radiation belt. *Geom. and Aeronom., 27(3),* 424-427.

THE AMS COLLABORATION, 2000a. Protons in near Earth orbit. *Phys. Lett. B, 472,* 215-226.

THE AMS COLLABORATION, 2000b. Leptons in near Earth's orbit. *Phys. Lett. B, 484,* 10-17.

YUAN, L. C. L. and C-S. WU, 1961. Fundamental Principles and Methods of Particle Detection, Academic Press, New York – London, 344.

A. A. Gusev[1], U. B. Jayanthi[1], V. M. Pankov[2], G. I. Pugacheva[3] and N.G. Schuch[3]

[1] Instituto Nacional de Pesquisas Espaciais, INPE, São Jose dos Campos, SP, Brasil
Email: anatoly@das.inpe.br
[2] Space Research Institute of Russian Academy of Science, Moscow, Russia
[3] Southern Regional Space Research Center/INPE, Santa Maria, Brazil